

Article

Facile Abatement of Oxygenated Volatile Organic Compounds via Hydrogen Co-Combustion over Pd/Al₂O₃ Catalyst as Onsite Heating Source

Lutf Ullah ^{1,2,†}, Sehrish Munsif ^{1,2,†}, Long Cao ^{1,2}, Jing-Cai Zhang ¹ and Wei-Zhen Li ^{1,2,*} 

¹ CAS Key Laboratory of Science and Technology on Applied Catalysis, Dalian Institute of Chemical Physics, Chinese Academy of Sciences, Dalian 116023, China; lutfikt77@dicp.ac.cn (L.U.); sehrish@dicp.ac.cn (S.M.); caolong@dicp.ac.cn (L.C.)

² University of Chinese Academy of Sciences, Beijing 100049, China

* Correspondence: weizhenli@dicp.ac.cn

† These authors contributed equally to this work.

Abstract: Catalytic combustion of volatile organic compounds (VOCs) usually requires external energy input to hold the desired reaction temperature via electric heating. This work presents an example of internal onsite heating of the catalytic active sites via hydrogen catalytic combustion with air over a conventional Pd/Al₂O₃ catalyst. Hydrogen combustion was ignited by the catalyst at room temperature without electric heating, and thus the temperatures were readily varied with the concentrations of H₂. Representative oxygenated VOCs such as methanol, formaldehyde and formic acid can be completely oxidized into CO₂ and water by co-feeding with H₂ below its low explosion limit of 4% using Pd/Al₂O₃ as shared catalyst. The catalytic performance apparently is not sensitive to the sizes of Pd nanoparticles in fresh and spent states, as revealed by XRD and STEM. This provides an option for using renewable green hydrogen to eliminate VOC pollutants in an energy-efficient way.

Keywords: catalytic H₂ combustion; volatile organic compounds; heating sources; Pd catalysts



Citation: Ullah, L.; Munsif, S.; Cao, L.; Zhang, J.-C.; Li, W.-Z. Facile Abatement of Oxygenated Volatile Organic Compounds via Hydrogen Co-Combustion over Pd/Al₂O₃ Catalyst as Onsite Heating Source. *Catalysts* **2024**, *14*, 372. <https://doi.org/10.3390/catal14060372>

Academic Editor: Guido Busca

Received: 23 May 2024

Revised: 5 June 2024

Accepted: 6 June 2024

Published: 10 June 2024

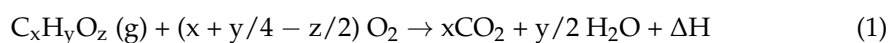


Copyright: © 2024 by the authors. Licensee MDPI, Basel, Switzerland. This article is an open access article distributed under the terms and conditions of the Creative Commons Attribution (CC BY) license (<https://creativecommons.org/licenses/by/4.0/>).

1. Introduction

Volatile organic compounds (VOCs) are a large group of carbon-based chemicals that evaporate easily at room temperature, including alkanes, alcohols, ketones, aldehydes, aromatics, paraffins, olefins, and halogenated hydrocarbons [1,2]. They contribute both directly as substances toxic to the environment and indirectly as ozone/smog precursors, so the release of VOCs is controlled by increasingly stringent regulations [3–6]. The emission of VOCs can be controlled via recovery and destruction strategies. Techniques based on recovery include absorption, adsorption, membrane separation, and condensation. Common problems faced in the recovery processes are the expense of materials and operation/maintenance costs, including the secondary disposal of enriched VOCs and spent absorbents, adsorbents, and/or coolants [7]. The destruction processes allow for the conversion of VOCs into carbon dioxide and water and the release of reaction heat as shown in Equation (1) via thermal, catalytic, or biological oxidation. Thermal oxidation or thermal incineration is usually conducted at high temperatures (>1000 °C) by burning fuel with VOCs blended in so that it can burn off more than 99% of VOCs. The disadvantage is its high fuel consumption and undesirable byproducts such as dioxins [8]. Catalytic oxidation can convert VOCs into CO₂, water, and fewer byproducts in the presence of a suitable catalyst at much lower operating temperatures (250–500 °C) [9–11]. Catalytic performance strongly depends on the nature of the catalyst, such as its formula and structure and on the operating conditions used, such as the nature of VOC mixtures, VOCs and oxygen concentration, overall gas flow rate, temperature, and type of reactor [12,13]. The strongly

exothermic nature of VOC oxidation usually leads to inevitable formation of local “hot spots” near the catalytic active sites, resulting in the thermal degradation of the catalyst and the loss of the energy-saving benefit.



$$k = A e^{-E_a/RT} \quad (2)$$

Obviously, the core issue for VOCs elimination is the problem of energy savings. As a chemical reaction, both thermal oxidation and catalytic oxidation obey the well-known Arrhenius equation as shown in Equation (2). To achieve a desired rate constant (k), thermal oxidation offers high reaction temperature (T) with less change in the activation energy (E_a), while catalytic oxidation aims to lower the reaction temperature by minimizing the activation energy required by the catalyst. Both thermal incineration and catalytic oxidation require heat energy input to maintain the temperature for complete oxidation of VOCs. Temperature rather than heat is the key parameter for activating VOCs oxidation, so a novel method to improve heating efficiency would be highly helpful. Unlike flame heating for thermal incineration, electric heating of the catalyst and reactants is achieved via heat conduction from a high-temperature electric furnace. Hydrogen is highly reactive and can readily react with VOCs on the surface of the catalyst. This method raises the catalyst bed temperature for VOCs elimination without electric heating, simplifying the system and reducing energy consumption and NO_x byproducts. Hydrogen addition promotes catalytic co-combustion, enhancing VOCs oxidation by increasing reactive species and lowering activation energy. This innovative approach maintains catalytic activity and ensures continuous VOCs oxidation, combining the benefits of thermal incineration and catalytic oxidation using hydrogen co-combustion. How could we raise the catalyst to the highest temperature in a catalytic oxidation process? Could hotspots over the catalyst be intentionally generated and utilized as ignitors for oxidation of VOCs?

Hydrogen is an advantageous fuel, as its combustion can provide efficient and eco-friendly energy [14]. Hydrogen combustion can yield an energy density of 142 MJ·kg⁻¹, surpassing the levels achieved by traditional hydrocarbon fuels [15]. If hydrogen combustion is to be adopted on a large scale, one effective approach to significantly reduce NO_x emissions in domestic applications would be through catalytic hydrogen combustion (CHC) with air [16]. Catalytic hydrogen combustion has been developed for heat and electricity generation with zero carbon-based emissions. It can start at room temperature with the use of noble metal catalysts such as supported Pd and Pt catalysts [13,17]. This provides an opportunity to use catalytic hydrogen combustion as an onsite heating resource by co-feeding with VOCs in the presence of noble metal catalyst. Pd/Al₂O₃ is a typical catalyst both for catalytic hydrogen combustion and for catalytic oxygenated VOCs combustion, potentially acting as a shared catalyst for co-combustion of hydrogen and VOCs.

In this work, we report a novel process that combines the benefits of thermal incineration and catalytic oxidation using hydrogen co-combustion over Pd/Al₂O₃ catalyst as heating source instead of classical electric heating. The catalytic combustion of H₂ over a Pd/Al₂O₃ catalyst can increase the temperature by heating the catalyst bed to levels at which VOCs such as methanol, formaldehyde, and formic acid can be completely oxidized, while maintaining the H₂ concentration below the lower explosive limit of 2–4%. The Pd/Al₂O₃ catalyst retains the igniting performance for H₂ combustion at room temperature albeit the size of Pd particles increased to ~20 nm after conducting the reaction around 900 °C. Such a simple and effective VOCs elimination system avoids energy-intensive external electric heating and provides a green utilization route of green H₂ from renewable energy.

2. Results

2.1. Structure Evolution of Pd/Al₂O₃ Catalyst

The Pd/Al₂O₃ catalysts before and after the catalytic oxidation of VOCs using H₂ co-combustion heating and electric heating were labeled as fresh and spent Pd/Al₂O₃ catalysts, respectively. The fresh Pd/Al₂O₃ sample had a high surface area of 202.7 m²/g, and the spent one remained at 114.5 m²/g, displaying unsurprising surface area decrease as usually reported. Figure 1 displays the XRD patterns for the fresh and spent Pd/Al₂O₃ catalysts. The fresh sample presented only the characteristic diffraction peaks for γ -Al₂O₃ and without peaks for Pd, indicating that the Pd was initially highly dispersed over the Al₂O₃ support. Two new peaks were observed at $2\theta = 33.8^\circ$ and 54.7° which were assigned to the diffraction for the (101) and (112) plane of PdO (JCPDF = 85-0713), respectively. The apparent crystallite size of PdO was determined to be about 23 nm using the Scherrer equation on the diffraction of (101). It is natural for PdO to form rather than metallic Pd, since the catalyst was cooled in air after terminating the reaction tests at a high temperature. Notably, the spent Pd/Al₂O₃ catalyst could still catalyze the hydrogen combustion at room temperature once hydrogen was introduced, although the metallic Pd small nanoparticles were oxidized into large PdO particles.

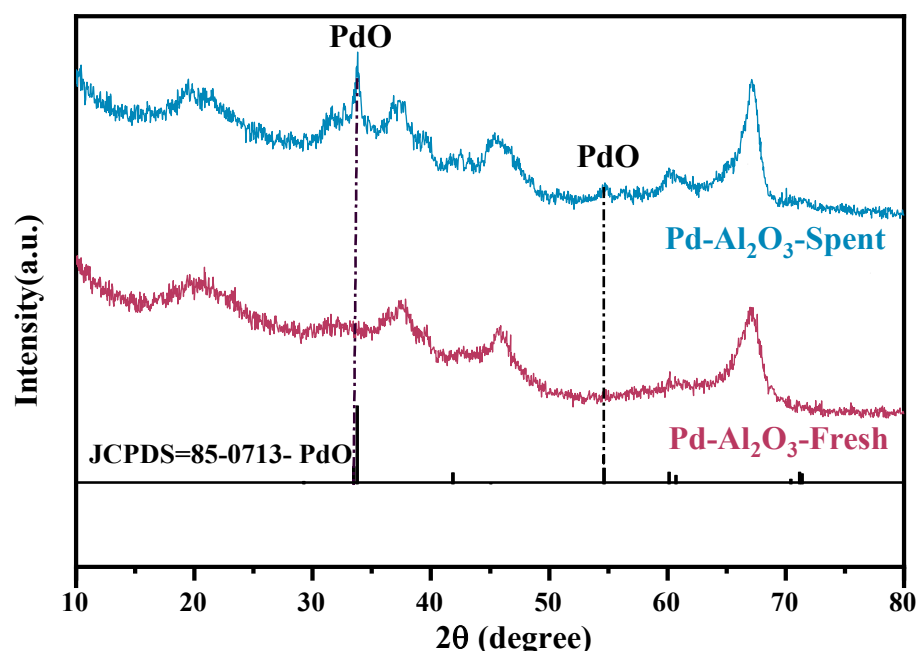


Figure 1. XRD patterns for fresh and spent Pd/Al₂O₃ catalysts.

The initial dispersion of Pd and the structural evolution after performance assessment were also addressed using HAADF imaging and element mapping. As shown in Figure 2a, the fresh Pd/Al₂O₃ sample had lots of small Pd nanoparticles with sizes of 3–6 nm, as circled in red. Besides the visible Pd particles, much smaller Pd species can be further evidenced from the element mapping image in Figure 2b. The scattered blue dots associated with Pd indicate the high dispersion of Pd over the Al₂O₃ support. For the spent Pd/Al₂O₃ catalyst, only a few large Pd particles of 10–40 nm in Figure 2c and sparse blue aggregations in Figure 2d are visible. Similar to the results reported in the literature, the sintering of Pd nanoparticles was inevitable and indeed happened for the conventional Pd/Al₂O₃ catalyst. Moreover, TEM images unambiguously reveal that both catalysts exhibit nanoparticle composed of Pd nanoparticles (Figure S1). Figure 3 presents the XPS spectra in the Pd 3d region for both fresh and spent Pd/Al₂O₃ catalysts, along with the fitting results of the signals. Moreover, X-ray photoelectron spectroscopy (XPS) was performed on the fresh and the spent samples to study the surface oxidation of Pd [18]. As shown in Figure 3, the Pd

spectrum shows positive shifts in binding energies, indicating the partial oxidation of Pd into PdO, consistent with XRD results.

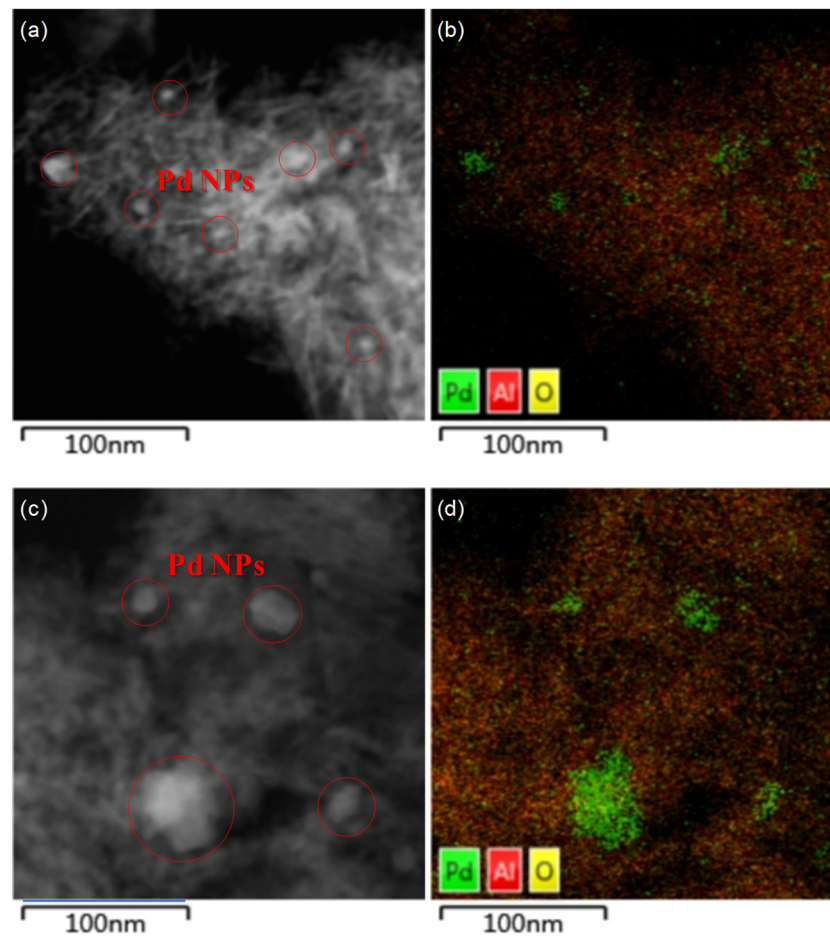


Figure 2. HAADF images and element mapping images for fresh (a,b) and spent (c,d) Pd/Al₂O₃ catalysts.

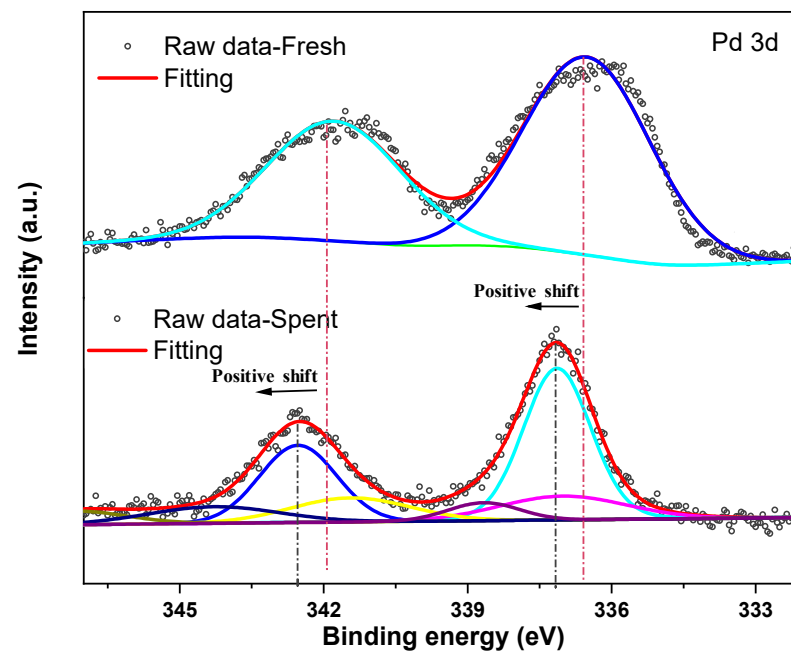


Figure 3. The XPS spectra of Pd on Pd/Al₂O₃ fresh and Pd/Al₂O₃.

2.2. Catalytic Performance Assessment

The purpose of using a Pd/Al₂O₃ catalyst is for the catalytic oxidation of H₂ and VOCs. First, we obtained the light-off temperatures for various VOCs over the fresh Pd/Al₂O₃ catalyst using temperature-programmed reactions on an electric heating furnace. Figure 4 displays the light-off curves, illustrated by CO₂ formation and the catalyst bed temperature raising profiles. For methanol, a jump of CO₂ signal happened on the stream at 28.5 min and a temperature of 190 °C. The CO₂ signal displays a peak from 28.5 min to 53.5 min, and the temperatures are also higher than those following the ramping slope, showing the exothermic nature of methanol combustion.

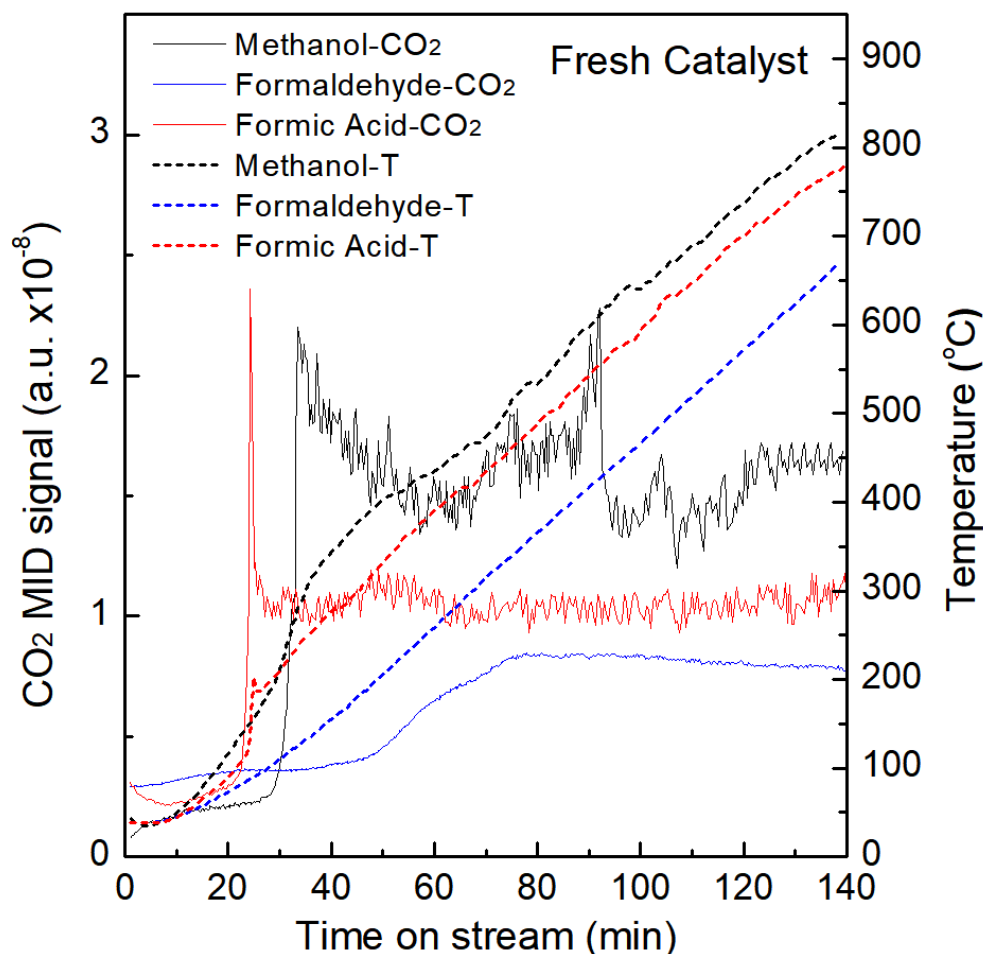


Figure 4. Light-off curves illustrated by CO₂ formation and catalyst bed temperature increase profiles during temperature-programmed reaction of methanol, formaldehyde, and formic acid over fresh Pd/Al₂O₃ catalyst using an electric heating furnace. The VOCs concentrations were controlled at 10% vapor, and the temperature ramping rate was 5 °C/min.

With further increases to the furnace temperature, the CO₂ signal reached a stable plateau over 700 °C, reflecting the complete oxidation of methanol. For formaldehyde, the CO₂ signal showed a slow increase from 48 min to 78 min, and the corresponding temperature from 200 °C to 350 °C. There was no obvious exothermic effect, possibly due to the very low formaldehyde volume concentration of ~0.02%. In the case of formic acid, a very sharp CO₂ peak occurred from 23.2 min to 26.2 min and a temperature peak from 110 °C to 185 °C. Such a sharp increase in the CO₂ signal indicates the existence of extra formic acid, possibly from the previously adsorbed formic acid on the catalyst's surface. In short, the light-off temperatures for methanol, formaldehyde and formic acid are 190 °C, 200 °C, and 110 °C, respectively.

The heating efficiency of catalytic combustion of H₂ over Pd/Al₂O₃ catalyst was evaluated by varying the H₂ concentrations under GHSV of 120,000 mL/(g-h). As shown in Figure 5, the catalyst bed temperature jumped from 20 °C to ~140 °C once 2% H₂ was introduced at room temperature [19]. The temperature could remain stable with flowing H₂. The temperature could reach and remain at ~200 °C when the H₂ concentration was increased to 3%. With a further elevation of the H₂ concentration to 4%, the temperature could remain at ~270 °C. Notably, the catalyst bed could be heated to temperatures higher than the light-off temperatures for methanol, formaldehyde and formic acid under H₂ concentrations below the low explosive limit (4%), showing great potential as a heating source as a substitute for electronic heating. Figure 6a shows the loading status of the Pd/Al₂O₃ catalyst and the position of the thermal couple in the quartz tube reactor. There was no visible change after the inlet of H₂ and 10% methanol vapor, while the top part of the loaded catalyst turned red after the methanol vapor reached 20%. When the methanol vapor reached 30%, more half than the upper part turned bright red, indicating the temperatures at the top are much higher than those at the bottom. The reason for this temperature gradient could be that the H₂ and air mixture reached the top first and quickly finished the exothermic combustion process, and then the produced hot gas heated the bottom. Indeed, the temperature measured using a thermal couple highly depended on its position, especially for reloaded samples for repeating experiments. Figure 6b displays the evolution profiles of CO₂ signals and catalyst bed temperatures with co-feeding of H₂ and VOCs. In this figure, the background CO₂ signals were collected by flowing air at 1000 mL/min for the first 20 min. The temperatures measured at 2% H₂ overlapped at 160 °C for the three VOCs tests, which was 20 °C higher than those measured in Figure 5, possibly due to the position change of the thermal couple during the reloading of the catalyst. For methanol, the temperatures displayed a stepwise jump from 160 °C to 450 °C, 695 °C, and 865 °C when methanol vapor of 10%, 20%, and 30%, i.e., the corresponding nominal methanol concentration of 1.3%, 2.6% and 3.9%, respectively, was co-fed with 2% H₂. At the same time, CO₂ signal intensities also increased to 2.5 a.u., 6.0 a.u., and 10.0 a.u. in stepwise mode. This temperature rise and CO₂ formation along with the inlet of methanol vapor indicate the co-combustion of methanol over the Pd/Al₂O₃ catalyst. For formaldehyde, the temperature increased slightly to 164 °C, 168 °C, and 173 °C when the formaldehyde vapor was at 10%, 20%, and 30%, respectively. Such a small temperature increase is possibly due to the low formaldehyde concentrations, i.e., 0.02%, 0.04%, and 0.06%, respectively. Thus, the corresponding CO₂ intensity was increased to 0.7, 0.9, and 1.2 at the beginning of the formaldehyde inlet. Notably, a slight decrease of CO₂ signal was detected with prolonged vapor flow, suggesting a possible incomplete conversion of formaldehyde. As for formic acid, it took about 17 min for the temperature and CO₂ to gradually reach their highest plateau after introducing 10% formic acid vapor. A stepwise increase in the temperatures and CO₂ signals were also observed when the formic acid vapor increased to 20% and 30%. The corresponding stable temperatures were 210 °C, 270 °C, and 335 °C, and the CO₂ signal intensities were 1.1, 2.3, and 3.5, respectively. Taken together, the oxidation of VOCs were indeed initiated by heating with hydrogen co-combustion catalyzed by a Pd/Al₂O₃ catalyst, although the preheated temperature using 2% H₂ (160 °C) was lower than the light-off temperatures of methanol (190 °C) and formaldehyde (200 °C). The profiles of CO₂ formation and temperature evolution for formaldehyde and formic acid are significantly different from that for methanol, possibly due to the much lower calorific values. As shown in Table 1, the calorific values of formaldehyde and formic acid with 10% vapor in the mixtures are only 5.1 and 58.8 kJ/m³, respectively, while that of the methanol mixture is 420.8 kJ/m³. The catalyst bed temperatures increased with the VOCs concentrations so that the self-heating effect further favored the catalytic oxidation performance. This phenomenon is very obvious for formic acid; i.e., the induction period which existed at 10% vapor content is not present any more at 20% and 30% vapor.

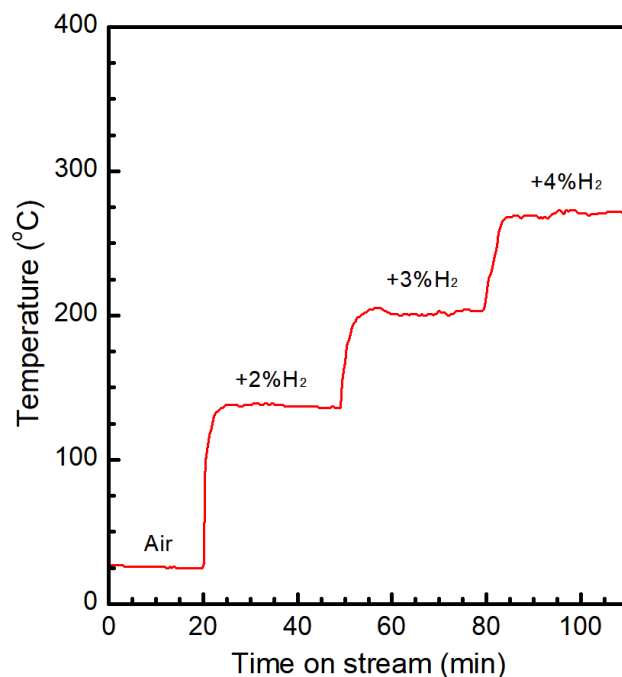


Figure 5. Temperatures of catalyst bed for 2%, 3%, and 4% H_2 in air with a total flow of 1000 mL/min over 0.5 g of Pd/ Al_2O_3 catalyst (GHSV: 120,000 mL/(h·g)).

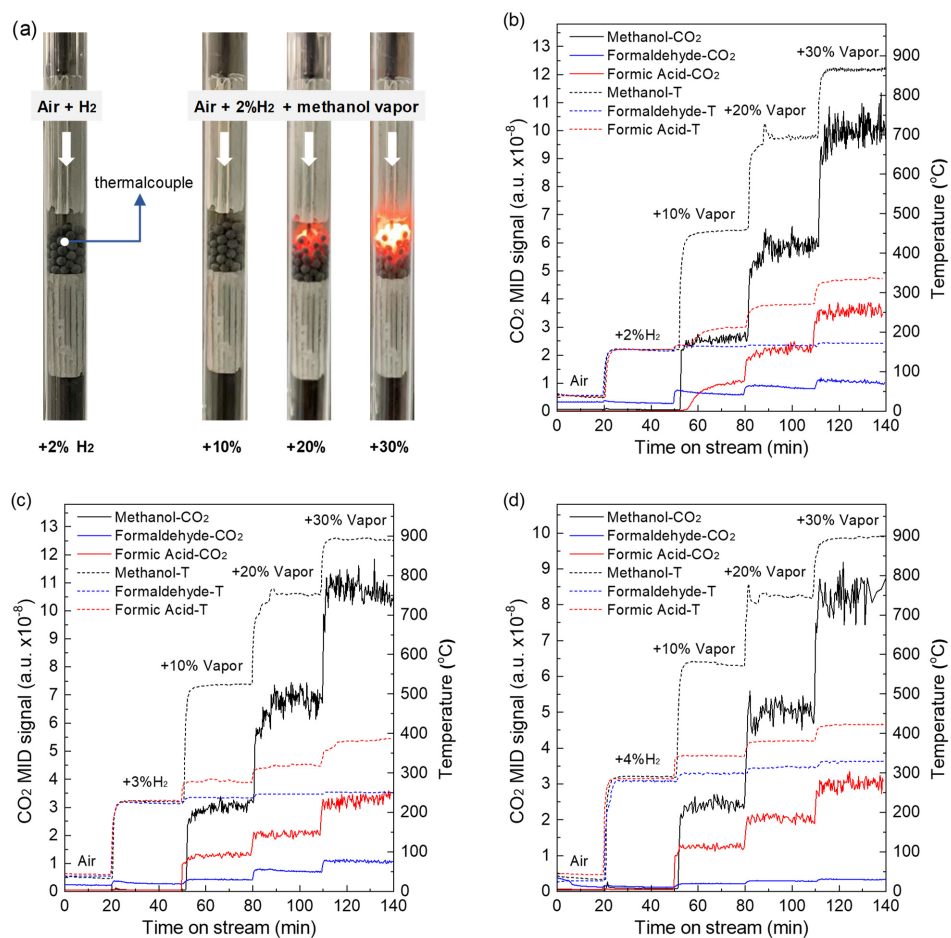


Figure 6. Pictures of the catalyst bed in the reactor under reaction conditions (a), and the CO_2 formation curves and the corresponding catalyst bed temperature profiles of various VOCs with co-combustion of H_2 of 2% (b), 3% (c), and 4% (d) over Pd/ Al_2O_3 catalyst.

Table 1. Vapor pressures and heat of combustion for various VOCs, and the nominal concentrations and calorific values for mixtures of VOCs and air in different compositions.

Chemical	Vapor Pressure (20 °C, kPa)	Heat of Combustion (25 °C, kJ/mol)	Nominal Concentration (%)			Calorific Value (kJ/m ³)		
			10% Vapor	20% Vapor	30% Vapor	10% Vapor	20% Vapor	30% Vapor
Hydrogen		286						
Methanol	13.0	725	1.3	2.6	3.9	420.8	841.5	1262.3
Formaldehyde	0.2 ^a	570.7	0.02	0.04	0.06	5.1	10.2	15.3
Formic Acid	4.6	254.6	0.5	0.9	1.4	56.8	102.3	159.1

^a Formaldehyde solution (30%).

Higher initial catalyst bed temperatures were achieved by elevating the H₂ concentrations to minimize the induction period. Figure 6c shows the CO₂ formation and the catalyst bed temperature evolution profiles when the co-feeding H₂ concentration was increased to 3%. The preheated temperature with 3% was 230 °C, which was increased by 70 °C compared to using 2% H₂. The temperatures for methanol oxidation jumped to 525 °C, 755 °C and 895 °C when methanol vapor was introduced at 10%, 20%, and 30% with 3% H₂. For formaldehyde and formic acid, the corresponding temperatures were 238 °C, 247 °C, 251 °C, and 280 °C, 320 °C, and 381 °C, respectively. All the temperature and CO₂ increases synchronously jumped dramatically without a slow induction period, indicating that the reaction temperatures were high enough for the VOCs' complete oxidation. With the further elevation of the H₂ concentration to 4% (Figure 6d), the preheated temperature reached 290 °C, which was 60 °C higher than when 3% H₂ was used. Accordingly, when the VOCs' vapor contents were 10%, 20%, and 30% in the mixture, the corresponding temperatures for methanol, formaldehyde, and formic acid were 580 °C, 750 °C, 895 °C, and 300 °C, 316 °C, 330 °C, and 345 °C, 380 °C, 425 °C, respectively. The instance response of CO₂ and catalyst bed temperature to the inlet of VOCs vapor and the holding at stable intensities together evidenced the complete oxidation of the VOCs.

2.3. Performance of Spent Catalyst

During the above catalyst performance assessments, the Pd/Al₂O₃ catalyst attained a high temperature of 895 °C in an oxygen-rich atmosphere. The spent catalyst demonstrated sintering characteristics such as decrease in surface area and aggregation of Pd and Al₂O₃ nanoparticles (Figures 1 and 2). The catalytic performance of the spent catalyst was evaluated relative to the light-off temperatures for various VOCs using temperature-programmed reactions on an electric heating furnace. As shown in Figure 7, a steep CO₂ rise was observed at 26.6 min where the light-off temperature was 150 °C for methanol over the spent Pd/Al₂O₃ catalyst, which was 40 °C lower than that over the fresh catalyst. For formaldehyde, two CO₂ peaks were observed at 150 °C and 360 °C while the peak was at 200 °C over the fresh catalyst. For formic acid, the light-off temperature was 150 °C, which is 40 °C higher than that over fresh catalyst. These results indicate that the spent catalysts are still highly active for catalyzing VOCs oxidation, in line with the fact that there was no detectable deactivation during the above H₂ and VOCs co-feeding tests.

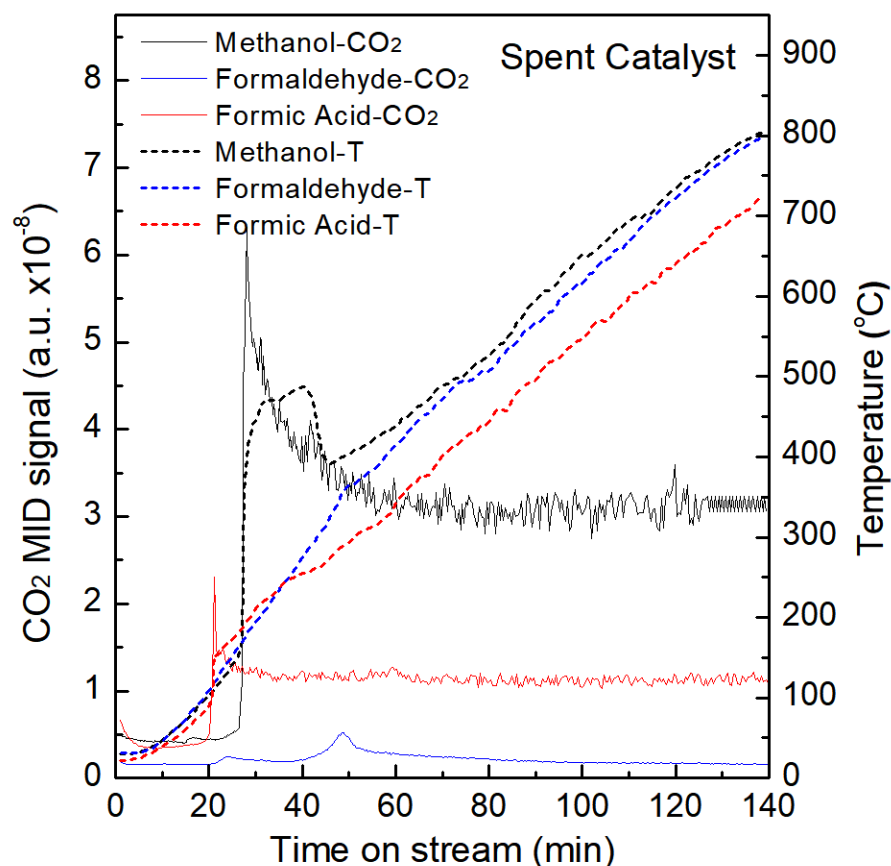


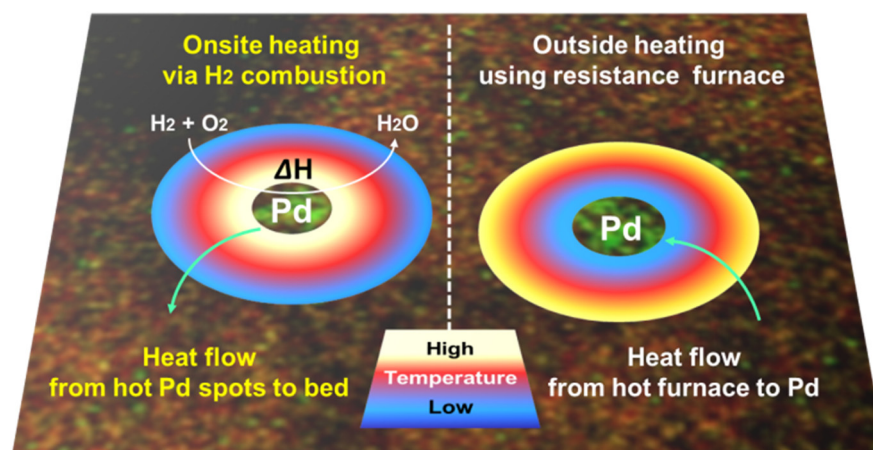
Figure 7. Light-off curves illustrated by CO₂ formation and catalyst bed temperature raising profiles during temperature-programmed reaction of methanol, formaldehyde, and formic acid over spent Pd/Al₂O₃ catalyst using an electric heating furnace. The VOCs concentrations were controlled at 10% vapor and the temperature ramping rate was 5 °C/min.

3. Discussion

3.1. Difference of Electric and Co-Combustion Heating Effect

Conventional electric heating on fixed-bed reactor usually adopts a resistance furnace which generates heat by the Joule effect in resistors located on the walls of the furnace chamber. The electrical energy transformed into heat in the resistors is used in part to raise the temperature of the reactor and in part to heat the walls of the chamber and to compensate for the furnace heat losses. The catalyst and gaseous reactants in the reactor are heated via radiation and conduction from an external hot furnace. As shown in the illustration Scheme 1, Pd sites are in the low-temperature region of the temperature gradient, indicating that only very tiny part of the electric heat energy was effectively used in the outside heating mode. For onsite heating via H₂ combustion, the heat generation and conduction are quite different. On the microscopic scale, H₂ and O₂ molecules are catalyzed by Pd/Al₂O₃ to react with each other at room temperature to form H₂O and release reaction heat. Due to its highly exothermic nature, the adiabatic flame temperature for hydrogen burning in air is 2127 °C, if no heat is lost in this process [20,21]. Notably, this temperature is extremely intense, and the highest temperature for Pd sites could be around 2000 °C, although the real temperature could be much lower due to inevitable heat exchange with the flowing air and produced water [22–24]. Taking particulate matter oxidation during diesel engine exhaust gas cleaning for reference, the temperature at the hot spot is approximately as high as 1000 °C [25]. Nevertheless, the Pd sites where the H₂ combustion happened become the hottest spots, and the reaction heat flow from Pd sites went elsewhere [20,26]. On the macroscopic scale, the catalyst bed presents a significant temperature gradient, decreasing from the top to the bottom, which is directly visible

in Figure 6a when more and more methanol was introduced together with H₂. The top 1/3 of the catalyst bed turned red at a temperature of 695 °C with the reactant mixture of air and 2% H₂ together with 20% methanol vapor, while the top half turned to bright red with temperature reaching 865 °C when the methanol vapor was increased to 30%. These results indicate that an exothermic combustion reaction occurred and was completed in the front part of the catalyst bed. Taken together, most of the chemical energy of H₂ was efficiently used to heat the catalytically active Pd sites to the highest temperature in the system. Co-combustion heating is much more energy-efficient than electric furnace heating, since there is no need to heat the whole reactor and the furnace.



Scheme 1. Illustration of onsite heating via H₂ combustion and outside heating using resistance furnace.

3.2. Benefits of Onsite Heating via H₂ Combustion in Catalytic Aspect

Catalytic combustion of H₂ over Pd/Al₂O₃ can start at room temperature. The catalytic function is highly retained even when the Pd/Al₂O₃ catalyst has suffered cyclic operation for various VOCs combustion at temperatures higher than 890 °C. This originates from the nature of Pd and seems not to be sensitive to the size of Pd particles, as the spent catalyst has much larger particles than the fresh one. This property allows Pd/Al₂O₃ to act as an ignitor for H₂ combustion at room temperature. Although the local temperature of Pd sites is not measurable in practice, it can be adjusted by controlling the reactant flow rate and the H₂ concentration. Apparently, the catalyst bed temperature could be raised by 60–70 °C per 1% H₂ at a total flow of 1000 mL/min at the top bed.

When the catalyst bed was heated with flowing H₂, the subsequently co-fed VOCs could also be involved in the catalytic combustion process. Taking methanol as example, a methanol molecule can be heated by exchanging heat with hot air and water before contact with hot Pd sites. The temperature of methanol and Pd sites can be easily adjusted by varying the H₂ and methanol concentrations. It is a pity that their respective temperatures are not measurable in practice, as the resulting catalyst bed temperature could also reflect the effect. For example, the bed temperature rose from 450 °C, 525 °C to 580 °C when the H₂ concentration increased from 2% to 3%, and 4% together with 10% methanol vapor. On the other hand, this also indicates that the combustion heat of methanol fed back and contributed to the bed temperature increase, further improving the oxidation reaction efficiency. Similar influences of H₂ and VOCs concentration on the VOCs conversions and bed temperatures were also demonstrated for formaldehyde and formic acid which have less calorific value, nevertheless the temperature rises of catalyst bed were indeed relatively much less. Onsite heating on the reactants and the active sites of catalyst were achieved simultaneously using a simple catalytic combustion of hydrogen over supported Pd catalyst. The Pd/Al₂O₃ acts as shared catalyst for both H₂ and VOCs combustion. The spent Pd/Al₂O₃ catalyst with coarse Pd particles retained enough catalytic capability to start H₂ combustion at room temperature and for completing VOCs combustion at elevated temperatures. The activity of both fresh and spent catalysts remained consistent despite

an increase in particle size and the oxidation of palladium in the spent catalyst due to the presence of sufficient amount of Pd nanoparticles in the catalyst.

4. Experimental Section

4.1. Catalyst Preparation

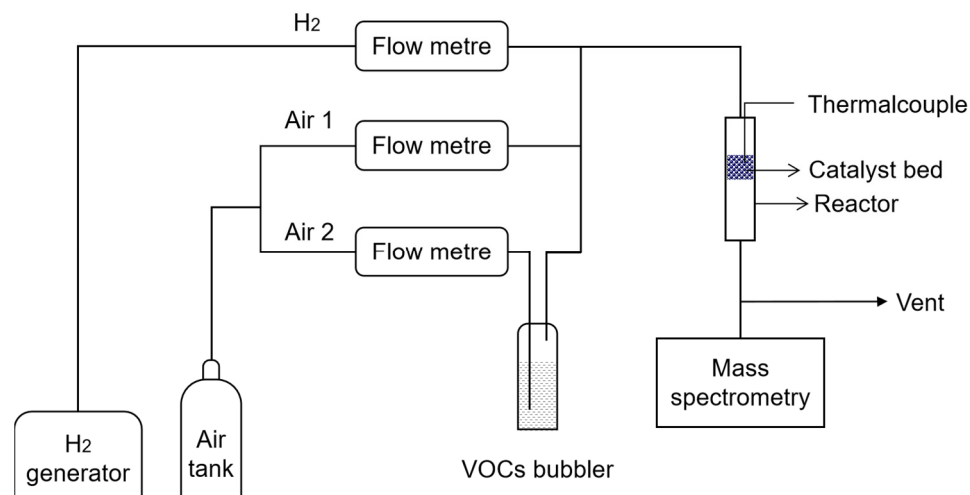
Pd/Al₂O₃ catalyst was prepared by incipient wetness impregnation of 100 g alumina (spherical shape in 2–3 mm, with 100 mL of PdCl₂ (Tianjin Fengchuan chemical reagent Technologies Co., Ltd. >99.9%, Tianjin, China) solution having Pd of 10 g/L to achieve Pd loading of 1 wt% on Alumina. The impregnated sample was dried at 120 °C for 8 h and then calcined at 500 °C for 5 h with a heating rate of 5 °C/min, and finally reduced in H₂ at 500 °C for 2 h with a flow rate of 300 mL/min.

4.2. Catalyst Characterizations

The specific surface areas of the fresh and spent catalysts were measured on a Micromeritics ASAP 2460 (Norcross, GA, USA) by N₂ adsorption at −196 °C using the Brunauer–Emmett–Teller (BET) analysis method. X-ray diffraction (XRD) patterns of the samples were recorded on a PANalytical PW 3040/60 X'Pert PRO diffractometer (Malvern, UK) equipped with a Cu K radiation source (=1.5406 Å), operating at 40 kV and 40 mA. Transmission electron microscopy (TEM) and scanning transmission electron microscopy (STEM) were performed on a JEOL JEM-2100F (Tokyo, Japan) at 200 keV. Energy dispersive X-ray spectroscopy (EDS) analysis was performed on an Oxford Instruments ISIS/INCA energy dispersive X-ray spectroscopy (EDS) system with an Oxford Pentafet Ultrathin Window (UTW) Detector (Abingdon, UK). Specimens were prepared by depositing a suspension of the powdered sample onto a lacy carbon-coated copper grid. X-ray photoelectron spectroscopy (XPS) measurements were performed using an ESCALAB 250 instrument equipped with Al K α radiation ($h\nu = 1486.6$ eV) (Waltham, MA, USA). The binding energy values were calibrated with the C 1s peak set at 284.6 eV.

4.3. Reactor Setup and Performance Test

The reaction setup is illustrated in Scheme 2. A quartz tube with an inner diameter of 10 mm and a length of 30 cm was used as the fixed-bed reactor. A 0.5 g quantity of Pd/Al₂O₃ catalyst having 0.78 cm³ was supported in the middle of the quartz tube by ceramic honeycomb (200 mesh). A k-type thermocouple was inserted into the catalyst bed to measure the temperature. Methanol, formaldehyde, and formic acid were chosen as representative molecular for alcohols, aldehydes, and acids. VOCs emissions were simulated by bubbling the chemical (methanol 99.7%, formaldehyde 30%, formic acid 99.7%, Tianjin Fuyu Fine Chemicals, Tianjin, China) vapor using flowing air at 100, 200, and 300 mL/min, respectively. Accordingly, the vapor concentrations in a total flow of 1000 mL/min were labeled as 10% vapor, 20% vapor, and 30% vapor. Table 1 lists the nominal concentrations and calorific values for mixtures of VOCs and air in different compositions. The nominal volume concentrations of methanol are 1.3%, 2.6% and 3.9%, and those for formaldehyde are 0.02%, 0.04% and 0.06%, and those for formic acid are 0.5%, 0.9% and 1.4%. Accordingly, the calorific values for the corresponding mixtures were estimated based on the heat of combustion and the VOCs content. Hydrogen was supplied by a high-purity hydrogen generator (Beijing Zhonghui, SPH-300A, Beijing, China). The flow rates of air and H₂ were controlled by calibrated mass flow controllers, and the total flow rate was maintained at 1000 mL/min, i.e., giving the gas an hourly space velocity of 120,000 mL/g-h or 77,000 h^{−1}. The reactants and products were analyzed and recorded using mass spectrometer Hiden Analytical (HPR-20, R&D) (Warrington, UK) by monitoring the signals of H₂ ($m/z = 2$), methanol ($m/z = 31$), formaldehyde ($m/z = 30$), formic acid ($m/z = 46$), and CO₂ ($m/z = 44$). Temperature-programmed catalytic reaction of VOCs and air over Pd/Al₂O₃ was conducted to identify the light-off temperatures using an electric heating furnace at a ramp rate of 5 °C/min from room temperature to 750 °C.



Scheme 2. Schematic diagram of VOCs combustion setup.

5. Conclusions

In summary, this work presents an example for catalytic combustion of oxygenated VOCs using hydrogen co-combustion over Pd/Al₂O₃ catalyst as a heating source instead of classical electric heating. This approach, despite lacking thermal recovery efficiency, offers low fuel costs and high oxidation efficiency. Consequently, the combustion of VOCs can be achieved more effectively than with traditional electric heating methods. Hydrogen combustion with air over a Pd/Al₂O₃ catalyst can begin at room temperature and release chemical energy as heat, although the size of Pd particles grew up to ~20 nm after conducting reaction around 900 °C. The catalyst bed and co-fed VOCs can be heated to the desired temperatures for complete combustion of representative VOCs such as methanol, formaldehyde, and formic acid by simply adjusting the H₂ concentration below the low explosive limit. This onsite heating manner using H₂ co-combustion avoids the use of resistance furnace, displaying great potential in energy and instrument cost saving. This work provides a way to combine the utilization of renewable green hydrogen energy and the elimination of VOCs pollutants.

Supplementary Materials: The following supporting information can be downloaded at: <https://www.mdpi.com/article/10.3390/catal14060372/s1>. Figure S1: HRTEM images for fresh (a,b,c) and spent (d,e,f) Pd/Al₂O₃ catalysts.

Author Contributions: L.U. and S.M. synthesized the catalysts and performed most of the experiments, collected and analyzed the data. L.C. and J.-C.Z. established the reaction setup and validated the concept. W.-Z.L. designed the study and supervised the project. All authors contributed to the general discussion and co-wrote the manuscript. All authors have read and agreed to the published version of the manuscript.

Funding: This work was supported by the “Transformational Technologies for Clean Energy and Demonstration”, Strategic Priority Research Program of the Chinese Academy of Sciences, (XDA21040200).

Data Availability Statement: Data presented in this article is available either in the main Manuscript, Supplementary Information or on reasonable request from corresponding author.

Conflicts of Interest: The authors declare that they have no conflicts of interest.

References

- Li, W.; Wang, J.; Gong, H. Catalytic combustion of VOCs on non-noble metal catalysts. *Catal. Today* **2009**, *148*, 81–87. [[CrossRef](#)]
- Peng, H.; Dong, T.; Yang, S.; Chen, H.; Yang, Z.; Liu, W.; He, C.; Wu, P.; Tian, J.; Peng, Y. Intra-crystalline mesoporous zeolite encapsulation-derived thermally robust metal nanocatalyst in deep oxidation of light alkanes. *Nat. Commun.* **2022**, *13*, 295. [[CrossRef](#)] [[PubMed](#)]
- Finlayson-Pitts, B.J.; Pitts, J.N., Jr. Tropospheric air pollution: Ozone, airborne toxics, polycyclic aromatic hydrocarbons, and particles. *Science* **1997**, *276*, 1045–1051. [[CrossRef](#)] [[PubMed](#)]

4. Rodhe, H. A comparison of the contribution of various gases to the greenhouse effect. *Science* **1990**, *248*, 1217–1219. [[CrossRef](#)] [[PubMed](#)]
5. Velinova, R.; Naydenov, A.; Kichukova, D.; Tumbalev, V.; Atanasova, G.; Kovacheva, D.; Spassova, I. Highly Efficient RGO-Supported Pd Catalyst for Low Temperature Hydrocarbon Oxidation. *Catalysts* **2023**, *13*, 1224. [[CrossRef](#)]
6. Yang, Y.; Si, W.; Peng, Y.; Chen, J.; Wang, Y.; Chen, D.; Tian, Z.; Wang, J.; Li, J. Oxygen vacancy engineering on copper-manganese spinel surface for enhancing toluene catalytic combustion: A comparative study of acid treatment and alkali treatment. *Appl. Catal. B Environ.* **2024**, *340*, 123142. [[CrossRef](#)]
7. Kujawa, J.; Cerneaux, S.; Kujawski, W. Removal of hazardous volatile organic compounds from water by vacuum pervaporation with hydrophobic ceramic membranes. *J. Memb. Sci.* **2015**, *474*, 11–19. [[CrossRef](#)]
8. Moretti, E.C. Reduce VOC and HAP emissions. *Chem. Eng. Prog.* **2002**, *98*, 30–40.
9. Carabineiro, S.; Chen, X.; Martynyuk, O.; Bogdanchikova, N.; Avalos-Borja, M.; Pestryakov, A.; Tavares, P.; Órfão, J.; Pereira, M.F.R.; Figueiredo, J.L. Gold supported on metal oxides for volatile organic compounds total oxidation. *Catal. Today* **2015**, *244*, 103–114. [[CrossRef](#)]
10. Chen, M.; Qi, L.; Fan, L.; Zhou, R.; Zheng, X. Zirconium-pillared montmorillonite and their application in supported palladium catalysts for volatile organic compounds purification. *Mater. Lett.* **2008**, *62*, 3646–3648. [[CrossRef](#)]
11. Santos, V.P.; Carabineiro, S.A.; Tavares, P.B.; Pereira, M.F.; Órfão, J.J.; Figueiredo, J.L. Oxidation of CO, ethanol and toluene over TiO₂ supported noble metal catalysts. *Appl. Catal. B Environ.* **2010**, *99*, 198–205. [[CrossRef](#)]
12. Peng, J.; Wang, S. Performance and characterization of supported metal catalysts for complete oxidation of formaldehyde at low temperatures. *Appl. Catal. B Environ.* **2007**, *73*, 282–291. [[CrossRef](#)]
13. Lalik, E.; Drelinkiewicz, A.; Kosydar, R.; Rojek, W.; Machej, T.; Gurgul, J.; Szumelda, T.; Kołodziej, M.; Bielańska, E. Activity and deactivation of Pd/Al₂O₃ catalysts in hydrogen and oxygen recombination reaction; a role of alkali (Li, Cs) dopant. *Int. J. Hydrogen Energy* **2015**, *40*, 16127–16136. [[CrossRef](#)]
14. Kozhukhova, A.E.; du Preez, S.P.; Shuro, I.; Bessarabov, D.G. Preparation of a cartridge-type Pt/Al₂O₃ catalyst using a sputter deposition method for catalytic hydrogen combustion. *Energy Fuels* **2022**, *36*, 13911–13923. [[CrossRef](#)]
15. Kaisare, N.S.; Vlachos, D.G. A review on microcombustion: Fundamentals, devices and applications. *Prog. Energy Combust. Sci.* **2012**, *38*, 321–359. [[CrossRef](#)]
16. Kozhukhova, A.; du Preez, S.; Bessarabov, D. Development of Pt–Co/Al₂O₃ bimetallic catalyst and its evaluation in catalytic hydrogen combustion reaction. *Int. J. Hydrogen Energy* **2024**, *51*, 1079–1096. [[CrossRef](#)]
17. Lalik, E.; Kołodziej, M.; Kosydar, R.; Szumelda, T.; Drelinkiewicz, A. Hydrogen and oxygen reaction on SiO₂ and MoO₃ supported Pd–Pt catalysts. *Recycl. Catal.* **2015**, *2*, 27–35. [[CrossRef](#)]
18. Fertal, D.R.; Monai, M.; Proano, L.; Bukhovko, M.P.; Park, J.; Ding, Y.; Weckhuysen, B.M.; Banerjee, A.C. Calcination temperature effects on Pd/alumina catalysts: Particle size, surface species and activity in methane combustion. *Catal. Today* **2021**, *382*, 120–129. [[CrossRef](#)]
19. Ladacki, M.; Houser, T.J.; Roberts, R.W. The catalyzed low-temperature hydrogen-oxygen reaction. *J. Catal.* **1965**, *4*, 239–247. [[CrossRef](#)]
20. Schefer, R.; Robben, F.; Cheng, R. Catalyzed combustion of H₂/air mixtures in a flat-plate boundary layer: I. Experimental results. *Combust. Flame* **1980**, *38*, 51–63. [[CrossRef](#)]
21. Kozhukhova, A.; Du Preez, S.; Shuro, I.; Bessarabov, D. Development of a low purity aluminum alloy (Al₆₀82) anodization process and its application as a platinum-based catalyst in catalytic hydrogen combustion. *Surf. Coat. Technol.* **2020**, *404*, 126483. [[CrossRef](#)]
22. Kozhukhova, A.E.; du Preez, S.P.; Malakhov, A.A.; Bessarabov, D.G. A thermally conductive Pt/AAO catalyst for hydrogen passive autocatalytic recombination. *Catalysts* **2021**, *11*, 491. [[CrossRef](#)]
23. Haruta, M.; Souma, Y.; Sano, H. Catalytic combustion of hydrogen—II. An experimental investigation of fundamental conditions for burner design. *Int. J. Hydrogen Energy* **1982**, *7*, 729–736. [[CrossRef](#)]
24. Haruta, M.; Sano, H. Catalytic combustion of hydrogen—IV. Fabrication of prototype catalytic heaters and their operating properties. *Int. J. Hydrogen Energy* **1982**, *7*, 801–807. [[CrossRef](#)]
25. Kim, J.; Kim, C.; Choung, S.-J. Comparison studies on sintering phenomenon of diesel oxidation catalyst depending upon aging conditions. *Catal. Today* **2012**, *185*, 296–301. [[CrossRef](#)]
26. Saint-Just, J.; Der Kinderen, J. Catalytic combustion: From reaction mechanism to commercial applications. *Catal. Today* **1996**, *29*, 387–395. [[CrossRef](#)]

Disclaimer/Publisher’s Note: The statements, opinions and data contained in all publications are solely those of the individual author(s) and contributor(s) and not of MDPI and/or the editor(s). MDPI and/or the editor(s) disclaim responsibility for any injury to people or property resulting from any ideas, methods, instructions or products referred to in the content.